Lantanida Journal, 14(2): 166-183 e-ISSN: 2548-9062 p-ISSN: 2356-3133

STRUCTURAL AND ELECTROCHEMICAL PROPERTIES OF CHITOSAN/GQDS/ZIF-67 COMPOSITES

Nessa Gina Sonia[1], Irwana Nainggolan[2*], Andriayani[2]
[1]Postgraduate School, Department of Chemistry, Faculty of Mathematics and Natural Science, Universitas Sumatera Utara, Medan, 20155, Indonesia
[2]Department of Chemistry, Faculty of Mathematics and Natural Science, Universitas Sumatera Utara, Medan, 20155, Indonesia
*Email: irwana@usu.ac.id

Article History: *Received: May 23, 2026* *Revised: June 25, 2026*
Accepted: June 29, 2026 *Published: July 31, 2026*

DOI: https://doi.org/10.22373/lj.v14i2.35174

ABSTRACT

The development of materials based on Zeolitic Imidazolate Framework-67 (ZIF-67) has attracted attention in the field of electrochemical sensors due to their large surface area, good porosity, and the presence of Co^{2+} active sites, which play a role in enhancing electrochemical activity and electron transfer at the sensor surface. To improve the stability and conductivity of these materials, ZIF-67 is combined with biopolymers and carbon nanomaterials to form functional composites with optimized sensor performance. In this study, chitosan/graphene quantum dots/ZIF-67 (CS/GQDs/ZIF-67) composites were successfully synthesized via stirring and ultrasonication-assisted mixing. Variations in ZIF-67 concentration were tested at 500, 1000, 1500, 2000, and 2500 mg/L to determine the optimal composition for electrochemical response. At the same time, electrochemical properties were analyzed by cyclic voltammetry (CV). XRD analysis revealed the formation of a crystalline structure in the CS/GQDs/ZIF-67 composite. Interactions among the components in the composite were confirmed through FTIR analysis. Meanwhile, FE-SEM results showed that the surface morphology had become more homogeneous, and EDX analysis confirmed the presence of Co, C, O, and N in the composite structure. CV testing showed that increasing the scan rate increased the anodic peak current, with the optimum scan rate at 125 mV/s. In addition, the optimal ZIF-67 concentration was 1500 mg/L, yielding the highest anodic peak current of 1.0466 x 10^{-4} A, indicating enhanced electrochemical activity and electron transfer. Overall, the CS/GQDs/ZIF-67 composite shows good potential as an electrode modification material for the development of cyclic voltammetry-based electrochemical sensors.

Keywords: chitosan, electrochemical sensor, graphene quantum dots, zeolitic imidazolate framework-67

INTRODUCTION

Electrochemical sensors are among the most widely used types of sensors today due to their numerous advantages, including extremely low detection limits down to the picomolar range, fast analysis times, and relatively low-cost instrumentation. The primary function of a chemical sensor is to provide accurate, real-time information about the chemical composition of its surroundings. In electrochemical sensors, analytical information is obtained from electrical signals generated through the interaction between the target analyte and the recognition layer on the sensor surface (Baranwal et al., 2022).

Cyclic voltammetry (CV) is an electrochemical method widely used in sensor development because it offers high sensitivity, fast response times, and information on electrochemical processes occurring at the electrode surface (Nainggolan, Martina, et al., 2024). CV employs a three-electrode system comprising a working electrode (WE), a reference electrode (RE), and a counter electrode (CE) (Dalal et al., 2023). This study focuses on the WE, the primary electrode where redox reactions occur (Adeniji & Stine, 2023). Copper-Printed Circuit Board (Cu-PCB) have been used in electrochemical applications. Cu-PCBs offer several advantages, including a simple and low-cost fabrication process, good corrosion resistance, and light weight. Although glassy carbon electrodes (GCE) are widely used as standard electrodes due to their good electrochemical stability, the performance of Cu-PCB can be enhanced through surface modification using functional materials. Therefore, the selection and understanding of the properties of the constituent materials are important factors in determining the sensor's electrochemical response (Nainggolan, Agusnar, et al., 2024; Ajibade & Oloyede, 2022).

Often referred to as coordination compounds, metal-organic frameworks (MOFs) symbolize a modern class of porous materials that have attracted considerable attention from academics. Zeolitic Imidazolate Framework-67 (ZIF-67) is one such material that is composed of cobalt ions (Co^{2+}) linked to 2-methylimidazolate ligands. ZIF-67 is an attractive material for electrochemical sensor applications because it exhibits good redox activity, high crystallinity, a microporous structure, a large specific surface area, and good chemical stability. In addition, its magnetic properties can help reduce interference during the detection process (Garg et al., 2020). ZIF-67 exhibits excellent redox properties in electrochemical sensors. This characteristic makes ZIF-67 suitable as a coating for Cu-PCB to enhance sensitivity. Sun et al., (2020) prepared graphene nanosheets coated with PA-ZIF-67@GS, which significantly enhanced the sensitivity of non-enzymatic electrochemical

glucose measurements in human blood serum. Although promising, ZIF-67 does not exhibit good conductivity, so it is hybridized with conductive materials (Ghafoor et al., 2023). The development of materials by incorporating substances such as carbon into the ZIF-67 matrix is a key strategy. This approach will enhance electrochemical performance on a macroscopic scale and significantly expand the range of sensor applications. Combining the advantages of ZIF-67 with other structures, such as GQDs, is an effective approach for producing compounds with potentially superior performance (Y. Hu et al., 2023; Bibi et al., 2021).

Graphene quantum dots (GQDs) are carbon nanoparticles measuring less than 10 nm that exhibit low intrinsic toxicity and excellent chemical and thermal stability (Nesakumar et al., 2022). GQDs have broad application prospects in bioimaging, photoluminescence, catalysis, and fluorescence sensing thanks to their high fluorescence efficiency, good water solubility, high specific surface area, superior electrical conductivity, high mobility, and good biocompatibility (Balkanloo et al., 2023). Furthermore, GQDs are good electron donors and acceptors, making them a promising material. This combination of properties makes GQDs an excellent transducer material in the design of electrochemical sensors (Chen et al., 2025). Research conducted by Sami Ben Aoun shows that N-GQDs–chitosan hybrids modified on nanostructured carbon electrodes have strong potential to improve the performance of electrochemical sensors for dopamine detection (Ben Aoun, 2017). Combining ZIF-67 with GQDs can enhance its conductivity and structural stability. GQDs can also covalently interact with 2-methylimidazole in ZIF-67 via π–π interactions (Thai et al., 2023). However, another challenge arises with the suboptimal adhesion of ZIF-67/GQDs, necessitating the use of additional materials to address it.

Chitosan (CS) is a chemically versatile polymer widely used in various applications due to its unique physicochemical properties, including low toxicity, biocompatibility, high adsorption capacity, and its good film-forming properties make it a suitable matrix for producing stable and homogeneous composites. These characteristics also provide advantages such as low cost, high accuracy, and practical applicability, while enhancing its mechanical properties (Nasution et al., 2018; T. Hu et al., 2022). Compared to other biopolymers, chitosan is a natural biopolymer with a very high content of free -NH_2 groups, unlike other biopolymers such as cellulose, starch, or lignin (which are generally dominated by hydroxyl (-OH) groups). The presence of these groups provides more active sites that can interact with metal ions through coordination or electrostatic interactions (Alemu et al., 2023). Indeed, this polycationic polysaccharide's multiple functional groups can be modified

with various ligands. In addition, -NH_2 groups are available for various chemical reactions, including reactions with aldehydes and ketones (Schiff base), metal chelation, alkylation, sulfonation, carboxymethylation, acetylation, grafting, quaternization, etc. Numerous hydroxyl (-OH) groups, as found in all polysaccharides, are available for chemical modification, such as sulfonation, carboxymethylation, phosphorylation, or hydroxyethylation. All chemical groups along the main chain can be cross-linked using specific agents to produce chemical hydrogels (Brasselet et al., 2019). Nainggolan have reported on working electrodes modified with CS/rGO/MnO_2 for cholesterol detection, noting that the sensitivity and reactivity of the chitosan-based thin-film working electrodes increased following modification (Nainggolan, Martina, et al., 2024).

As a promising material, a combination of chitosan (CS), graphene quantum dots (GQDs), and ZIF-67 were prepared via stirring and ultrasonication-assisted mixing. This combination of the three components is expected to enhance sensor performance, particularly by improving electrochemical response. Therefore, this study focuses on the development of a simple, cost-effective electrochemical sensor by modifying a working electrode with the CS/GQDs/ZIF-67 composite.

RESEARCH METHODS

Chemicals, Equipment, and Instrumentation

All reagents used are commercially available, such as CS of medium molecular weight (Sigma-Aldrich), ZIF-67 (NRE), GQDs (Sigma-Aldrich), aquadest, glacial acetic acid (CH_3COOH), ethanol p.a, phosphate buffer saline (PBS) pH 7, deionized water (DI), Copper-Printed Circuit Board (Cu-PCB) substrate. The first step involved dissolving CS, GQDs and ZIF-67. The equipment used includes an analytical balance (Mettler), oven (Memmert), hotplate stirrer (Cimarex), magnetic stir bar, ultrasonic bath (Kerry Pulsatron), power supply (OOCU), FT-IR system (Shimadzu IR Prestige-21) to identify the functional groups and investigate the chemical interactions within the composite material, FE-SEM system (Thermo Scientific Quattro S) to analyze the morphology of the electrode surface, XRD system (Bruker D8 Advance) as a technique to characterization the phase structures, and potentiostat (CorrTest) is used to evaluate the electrochemical properties of electrodes using cyclic voltammetry (CV) .

Preparation of CS/GQDs/ZIF-67

CS 1.5% (w/v) was dissolved in 2% acetic acid, while GQDs 250 mg/L were homogenised and sonicated at 20 Hz for 2 h. And ZIF-67 was dispersed in 50 mL of ethanol under stirring for 6 h at room temperature, then ultrasonicated for about 30 min to form a homogeneous dispersion. stirring and ultrasonication-assisted mixing are two methods selected for their simplicity and uniform outcomes. This was followed by the preparation of CS, CS/GQDs and CS/GQDs/ZIF-67 thin films. CS concentration of 1.5% (w/v), GQDs 250 mg/L, and varying concentrations of ZIF-67 (500, 1000, 1500, 2000, and 2500) mg/L were then mixed with the ratio 2:1:1 under constant stirring at 200–300 rpm for 24 hours until the mixture was mixed homogeneously, and followed by an ultrasonication process for 1 hour. CS, CS/GQDs, and CS/GQDs/ZIF-67 solutions were poured onto cleaned glass plates. The glass plates containing the solutions were dried in an oven at 60°C for 4 hours (Garg et al., 2020; Nainggolan, Martina, et al., 2024).

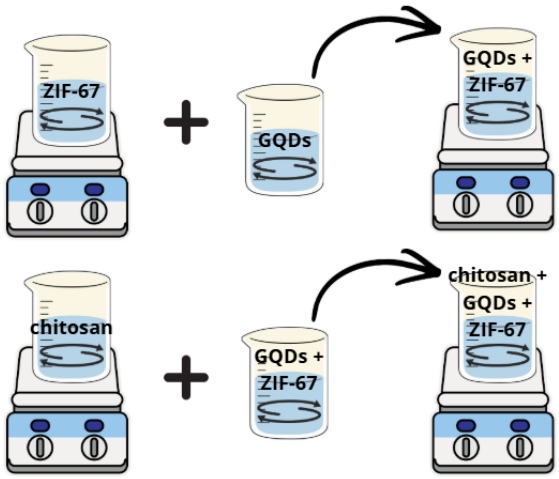

Figure 1. The Stirring Process of The CS/GQDs/ZIF-67 Solution

CS/GQDs/ZIF-67 film layer on a Copper-Printed Circuit Board (Cu-PCB) was prepared by electrodeposition. This technique was chosen because it can effectively deposit a thin layer of material onto the surface of the working electrode through an electrochemical reaction controlled by an applied electric current. This method allows for the deposition of various materials such as metals, metal oxides, and composites onto the electrode surface through electrochemical reactions in an electrolyte containing the target ions (Marathe et al., 2025; (Nainggolan et al., 2026).

During electrodeposition, the protonated amino groups (NH_3^+) of CS migrate toward the cathode, forming a uniformly deposited film. The deposition process was carried out by

applying a 3.6 V for 5 minutes. Subsequently, the PCB substrate modified was dried in an oven at 60°C for 60 minutes. The electrode modified with CS/GQDs/ZIF-67, obtained by electrodeposition, is shown in Figure 2.

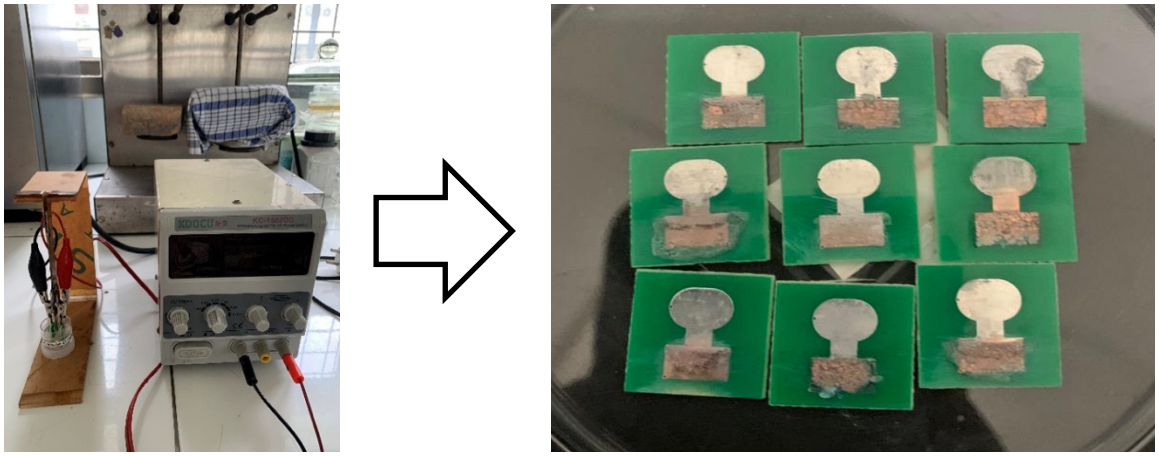

Figure 2. Electrodeposition Process of CS/GQDs/ZIF-67 Modified Copper Electrode

CS acts as a positively charged polyelectrolyte matrix that binds GQDs and ZIF-67 via electrostatic interactions and hydrogen bonding. When a negative potential is applied to the copper electrode, a water reduction reaction occurs, producing OH^- ions, thereby increasing the local pH around the cathode surface. This increase in basicity causes the NH_3^+ groups to deprotonate to neutral $–NH_2$ groups, leading to a loss of CS solubility and precipitation along with the GQDs and ZIF-67 particles. Consequently, a thin CS/GQDs/ZIF-67 composite layer forms on the working electrode surface (M. Liu et al., 2018).

RESULTS AND DISCUSSION

The CS/GQDs/ZIF-67 composite was successfully synthesized using stirring and ultrasonication-assisted mixing methods with varying concentrations of ZIF-67 to obtain the optimal composition. The success of composite formation and the interactions among its components were evaluated through a series of structural and morphological characterizations. XRD characterization was performed to identify the material's crystalline structure, while FTIR was used to confirm the presence of functional groups and chemical interactions among the composite's constituents. Furthermore, surface morphology and elemental distribution were analyzed using FE-SEM and EDX. After the physical characteristics of the material were confirmed, the electrochemical properties of the

composite were evaluated using cyclic voltammetry to examine the effect of ZIF-67 addition on electrochemical activity and electron transfer capability.

X-Ray Diffraction (XRD) Analysis

The crystal structure of the Chitosan/GQDs and Chitosan/GQDs/ZIF-67 films was characterized using X-ray diffraction (XRD) in the range of 10°–90°. The diffraction patterns consist of XRD spectra that show the relationship between the scattering angle (2θ) and the peak intensity of the spectrum.

The crystal structure of the compound CS/GQDs and CS/GQDs/ZIF-67 was analyzed using XRD characterization. In Figure 3, XRD patterns can be observed at peaks at 2θ° = 19.16° and 20.34°, which are attributed to hydrated CS crystals with hydrogen bonds between amino groups (Adeyemi & Ojoawo, 2023). At the peak at 2θ° = 26.64° corresponding to the plane of GQDs (Salehi et al., 2025). The XRD pattern of CS/GQDs/ZIF-67 at the peaks of 2θ° = 12.62°, 22.7°, and 24.94° indicates the presence of the ZIF-67 crystal structure with low intensity. Consistency of this XRD pattern with previ ous reports indicated the successful formation of the ZIF-67 crystal structure (Bakar et al., 2024).

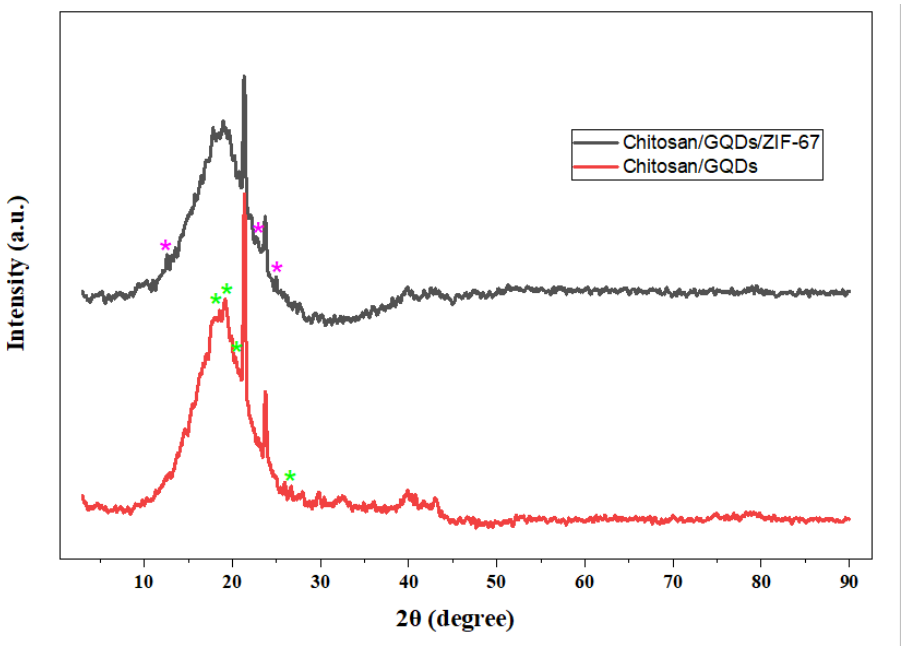

Figure 3. The XRD Spectra of CS/GQDs and CS/GQDs/ZIF-67

Fourier Transform Infrared Spectroscopy (FTIR) Analysis

The functional groups of CS/GQDs/ZIF-67 films were analyzed using FTIR spectroscopy. Thin films of CS, CS/GQDs, and CS/GQDs/ZIF-67 were used as test samples. During FTIR characterization, characteristic absorption bands observed in the transmittance spectra indicated the interaction of infrared radiation with molecular components at specific wavelengths. These bands are related to the vibrational behavior of chemical bonds within the material. CS, GQDs, and ZIF-67 were successfully mixed to form a homogeneous and stable solution at room temperature. The resulting chitosan, CS/GQDs, and CS/GQDs/ZIF-67 matrix was then cast into an acrylic mold and allowed to dry until a thin film formed. The FTIR spectra of the CS, CS/GQDs, and CS/GQDs/ZIF-67 thin films are shown in Figure 4.

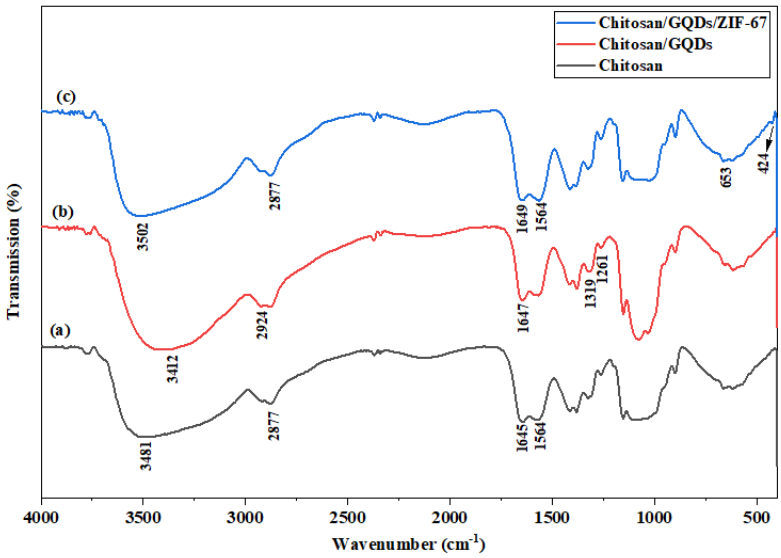

Figure 4. The FTIR Spectra of CS, CS/GQDs and CS/GQDs/ZIF-67

Fourier transform infrared (FTIR) spectra confirmed the interaction between CS, GQDs, and ZIF-67 in the CS, CS/GQDs, and CS/GQDs/ZIF-67. As shown in Figure 4, in spectrum (a), CS exhibits a distinct peak at a wavenumber of 3481 cm^{-1}, corresponding to the vibrational mode of the -OH group. At a wavenumber of 2877 cm^{-1}, there is a stretching vibration of the C-H bond in the -CH_2- group of the chitosan aliphatic chain. The wavenumber 1645 cm^{-1} represents the C=O peak (amide I), and the wavenumber 1564 cm^{-1} indicates the bending vibration of the N-H bond (amide II) (Amari et al., 2021). In the spectrum of (b) Chitosan/GQDs exhibit a broad absorption band associated with stretching vibrations between the -OH/NH_2 groups of chitosan and the oxygen groups (C=O, COOH) on the GQDs, which shifts from 3481 cm^{-1} to 3412 cm^{-1} after the addition of GQDs. There

is a C-O-C stretching vibration at 1261 cm^{-1} and a C–H stretching vibration at approximately 2924 cm^{-1}.

The formation of hydrogen bonds between the CS amine groups and the GQDs carboxylate groups indicates the successful integration of the two materials into the composite (Esmaeilzadeh et al., 2020). (c) In the CS/GQDs/ZIF-67 composite, the wavenumber at 1647 cm^{-1} that is slightly shifted to 1649 cm^{-1}, indicating a coordination interaction between the chitosan -NH_2 groups and Co^{2+} ions. The peak at 1564 cm^{-1} represents the C=N stretching vibration of 2-methylimidazole, indicating the presence of ZIF-67 (Shahzaib et al., 2024). While the peaks at 1413 cm^{-1} and 1263 cm^{-1} are associated with the stretching and bending vibrations of the imidazole. In addition, the band at 424 cm^{-1} is allocated to the Co–N band in case of CS/GQDs/ZIF-67 (Zhang et al., 2024).

Field Emission Scanning Electron Microscopy Analysis

Surface morphological characterization using Field Emission-Scanning Electron Microscopy (FE-SEM) was performed on the Chitosan, Chitosan/GQDs, and Chitosan/GQDs/ZIF-67 layers at specific magnifications.

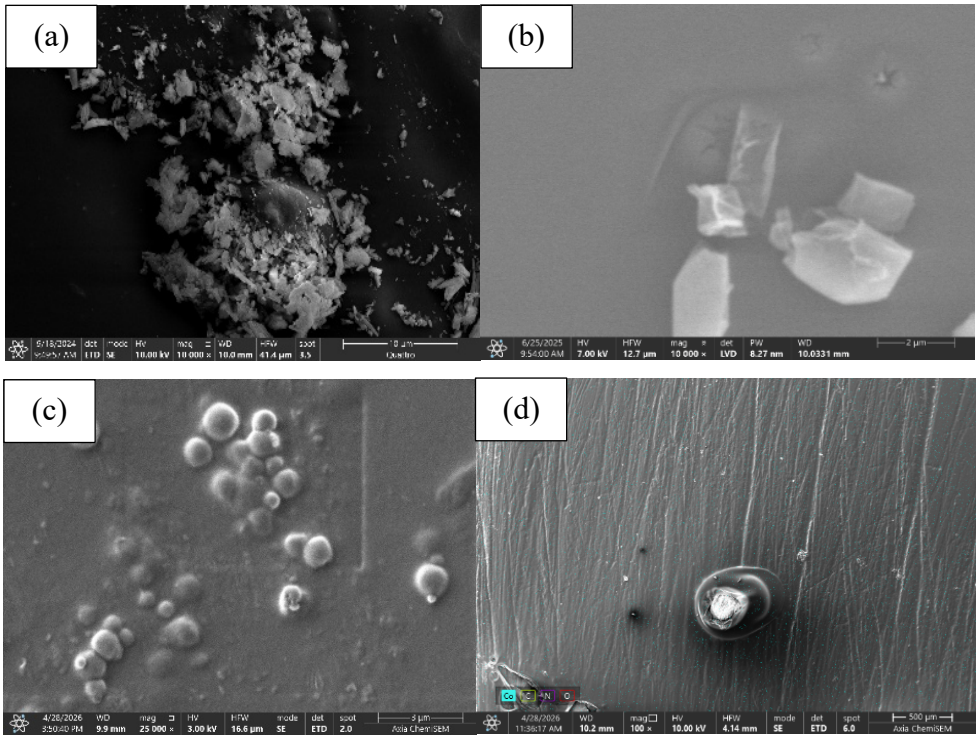

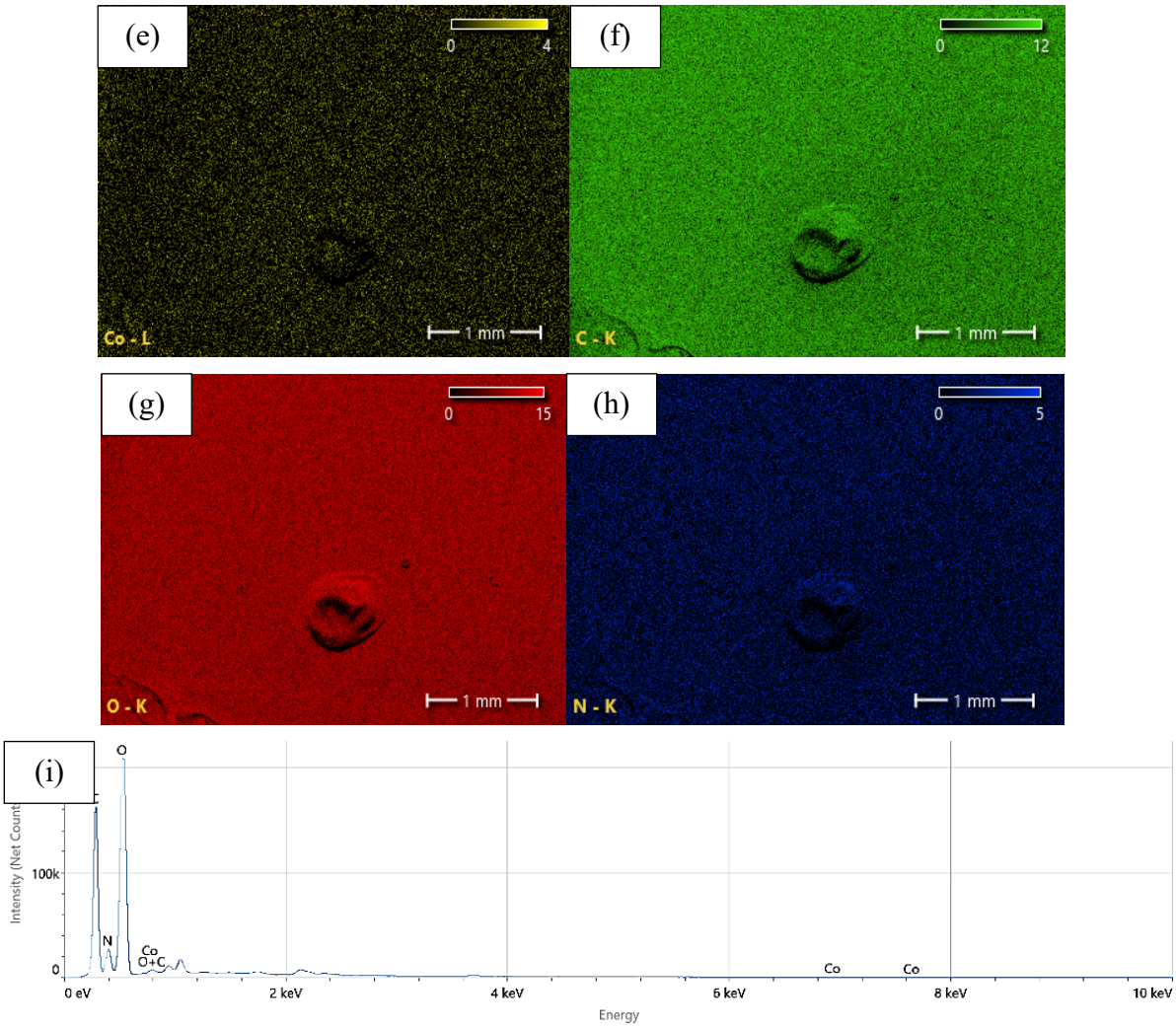

Figure 5. FE-SEM Micrographs of (a) CS, (b) CS/GQDs, (c) CS/GQDs/ZIF-67, (d-h) Elemental mapping patterns of the CS/GQDs/ZIF-67 Co, C, O, N, (i) EDX spectrum of as prepared CS/GQDs/ZIF-67

Table 1. EDX spectrum of as prepared CS/GQDs/ZIF-67

Elements	Line	At. %	Wt. %	Net Counts	At. % Error	Wt. % Error
C	K	31.4	25.1	883 894	0.1	0.1
N	K	6.7	6.3	106 706	0.1	0.1
O	K	60.9	64.8	1 237 274	0.3	0.3
Co	L	1.0	3.8	21 193	0.0	0.1

According to Figure 5 (a), the CS surface exhibits a morphology consisting of a rough layer with few pores. This structure forms due to CS tendency to naturally aggregate in solution. (b) CS/GQDs appear as irregular particles in the form of flakes and small blocks that have agglomerated to form aggregates (Sarhan et al., 2022). Partial interactions between

CS and GQDs result in a rod-shaped (nanorod) structure. (c) chitosan/GQDs/ZIF-67: It appears that ZIF-67 has successfully integrated with chitosan/GQDs; after mixing with ZIF-67, the surface becomes rougher due to the adhesion of ZIF-67 nanoparticles (L. Liu et al., 2019). (d-i) In this study, the presence of each expected element, such as Co, C, O, and N in the structure, was confirmed using energy-dispersive EDX.

Cyclic Voltammetry (CV) Analysis

The electrochemical properties of chitosan/GQDs/ZIF-67-based electrodes were evaluated using CV with a PBS solution at pH 7 which was used as a supporting electrolyte to assess the electrodes' intrinsic electrochemical response prior to testing with standard redox probes or target analytes. The use of PBS solution at pH 7 is consistent with previous reports on the electrochemical behavior of modified electrodes based on chitosan, GO/ZIF-67, MXene/MOF composites, and related nanostructured materials (Herbei et al., 2023; P et al., 2025; Shahsavari et al., 2022). Therefore, PBS at pH 7 was selected as the supporting electrolyte in this study to evaluate the effect of material modification on the electrode's electrochemical response.

The determination of the optimal scan rate on the CS/GQDs/ZIF-67-modified electrode. The scan rate was determined to observe its effect on the electron flow exchange rate. The effect of potential on the oxidation and reduction peak currents can influence the scan rate; a higher scan rate yields a larger reduction peak current. This determination can then be used as the optimal scan rate for the modified electrode. The following are the scan rate measurement results. In this measurement, a CS/GQDs/ZIF-67 solution deposited on a copper printed circuit board (Cu-PCB) substrate was used as the working electrode (WE), an Ag/AgCl reference electrode (RE), and a Pt counter electrode (CE). These three electrodes operated simultaneously to evaluate the optimal concentration of the CS/GQDs/ZIF-67 solution. As a preliminary test, scan rates of 25, 50, 75, 100, 125, and 150 mV/s were applied. Subsequently, the optimal concentration of the electrode modified with CS/GQDs/ZIF-67 was determined to characterize its electrochemical properties. Current measurements were performed within a potential range of −1 V to +1 V to obtain anodic (oxidation) and cathodic (reduction) responses.

Figure 6 shows the scan rate measurement results for the CS/GQDs/ZIF-67-modified electrode. Scan rate studies are crucial for understanding the redox reaction process, material stability, and performance. Variations in scan rate were conducted to observe the effects on

electron transfer kinetics and electrochemical response, evaluated based on the anodic (IpA) and cathodic (IpC) peak currents. As the scan rate increased, the values of IpA and IpC also increased. Although the peak currents increased with scan rate, the voltammogram at 125 mV/s showed the clearest and most stable oxidation and reduction peaks.

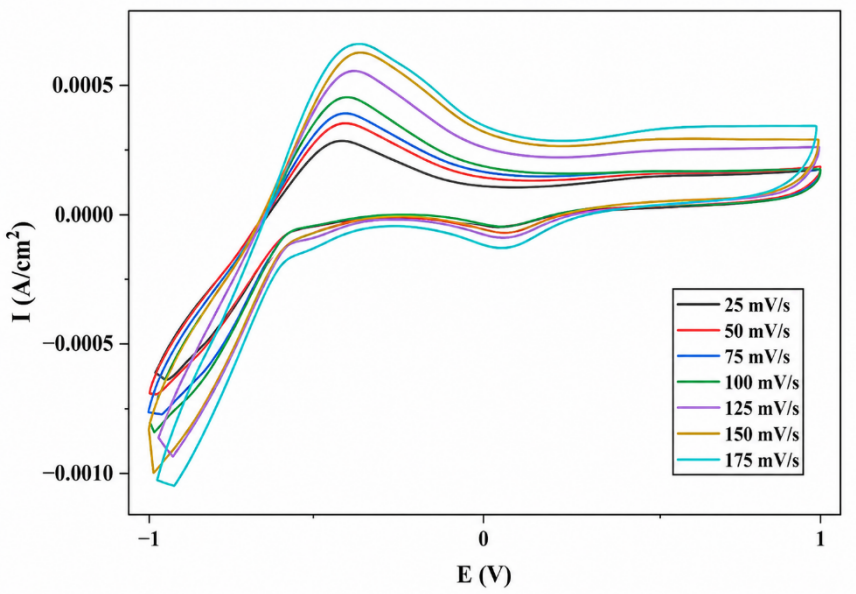

Figure 6. CV Curves of CS/GQDs/ZIF-67 of Scan Rate (25-175 mV/s) in PBS pH 7

An increase in the scan rate causes the anodic peak current to rise because electron transfer at the electrode surface occurs more rapidly. Conversely, a lower scan rate yields a thicker diffusion layer at the electrode surface, thereby hindering electron transfer and reducing the current response (Andani, 2017). However, if the scan rate is too high, incomplete electrochemical reactions occur because the interaction time with the analyte is too short. Conversely, if the scan rate is too low, it may trigger side reactions in the chitosan matrix. The relationship between the IpA value and the scan rate was analyzed to evaluate the electrochemical characteristics of the modified electrode. The results of the linear regression yielded the equation $y = 2.2979 \times 10^{-4} + 2.08894 \times 10^{-6} x$ with a coefficient of determination ($R^2 = 0.9904$), indicating an excellent linear correlation. High linearity indicates that the electrode's electrochemical response is significantly affected by changes in the scan rate. It should be noted that this analysis does not characterize the sensor's sensitivity, as determining sensitivity requires a calibration curve based on variations in analyte concentration. Rather, the results obtained provide insight into the electron transfer mechanism in the modified electrode system. Thus, this test is more appropriately used as a

basis for evaluating the electrode's response to the scan rate, rather than for quantitatively determining the sensor's performance.

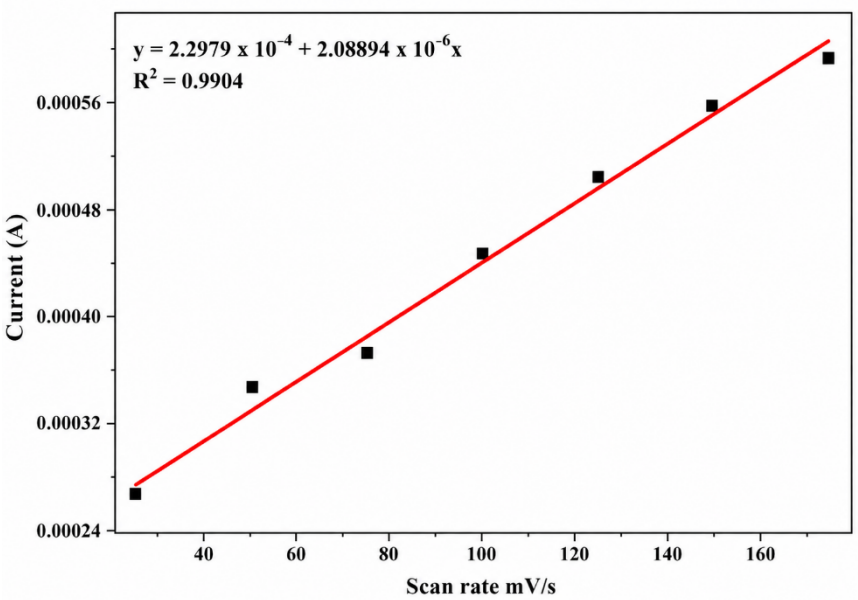

Figure 7. CV Curves of CS/GQDs/ZIF-67 at 25-175 mV/s in PBS pH 7

Table 2. Determination of Optimal Scan Rate Based On IpA and IpC Values

Scan rate (mV/s)	IpA (A)	IpC (A)
25	2.674×10^{-4}	-0.657×10^{-4}
50	3.484×10^{-4}	-0.613×10^{-4}
75	3.727×10^{-4}	-0.577×10^{-4}
100	4.418×10^{-4}	-0.736×10^{-4}
125	$\mathbf{4.992 \times 10^{-4}}$	$\mathbf{-1.027 \times 10^{-4}}$
150	5.494×10^{-4}	-0.985×10^{-4}
175	5.865×10^{-4}	-1.353×10^{-4}

The optimal concentration of the modified electrode was determined using cyclic voltammetry (CV) in phosphate-buffered saline (PBS) at pH 7. The aim was to determine the optimal composition of the Cu-PCB electrode modified with CS/GQDs/ZIF-67 and to identify the most suitable ZIF-67 content for further analysis. Figure 8 shows clear oxidation and reduction peak currents at each CS/GQDs/ZIF-67 concentration. The addition of varying amounts of ZIF-67 enhances the material's mechanical and electrical properties. In evaluating the optimal modified electrode, the anodic peak current (IpA) was used as the criterion. The anodic peak current (IpA) indicates the oxidation process at the electrode surface and is related to the electron-transfer efficiency and the active surface area of the modified electrode.

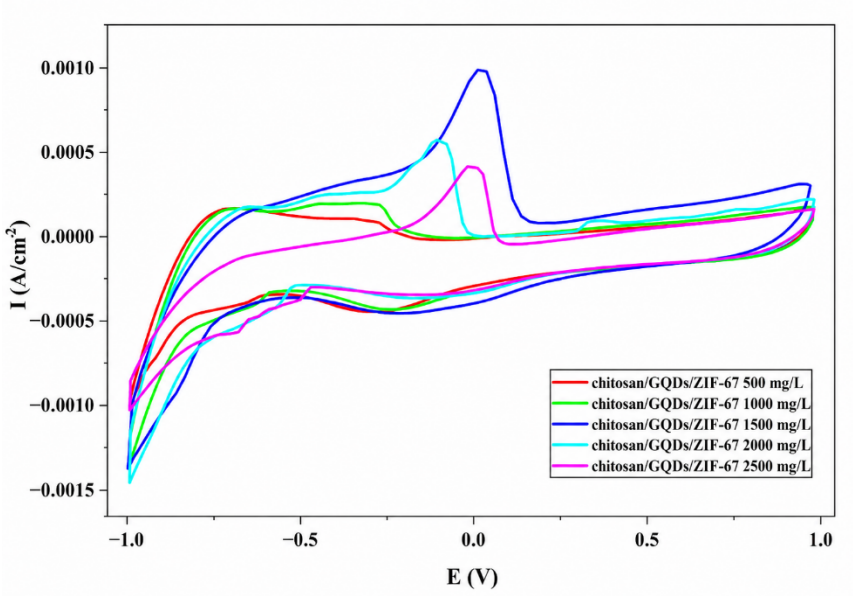

Figure 8. CV Curves of CS/GQDs/ZIF-67 Modified Electrode With Variation of ZIF-67 in PBS pH 7

Table 3. Determination of Optimum Electrode

ZIF-67 (mg/L)	EpA (V)	EpC (V)	IpA (A)	IpC (A)	ΔEp (V)	|IpA/IpC| (A)
500	-0.438	-0.236	0.3698×10^{-4}	-0.1621×10^{-4}	-0.202	2.281
1000	-0.685	-0.284	0.4287×10^{-4}	-0.1624×10^{-4}	-0.401	2.639
1500	**0.016**	**-0.217**	$\mathbf{1.0466 \times 10^{-4}}$	$\mathbf{-0.1561 \times 10^{-4}}$	**0.233**	**6.704**
2000	-0.107	-0.173	0.6821×10^{-4}	-0.1299×10^{-4}	0.066	5.250
2500	-0.009	-0.158	0.5469×10^{-4}	-0.0983×10^{-4}	0.149	5.563

As shown in Table 3, we can observe that the IpA value increases as the ZIF-67 concentration rises from 500 to 1500 mg/L, and then decreases at higher concentrations. The increase in the IpA value indicates that ZIF-67 is capable of enhancing electrochemical activity. This is related to the presence of Co^{2+} active sites, which facilitate faster electron transfer at the electrode surface. At a concentration of 1,500 mg/L, the highest IpA value was obtained, at 1.0033 mA. This indicates that a concentration of 1,500 mg/L contributes most effectively to the composite's electrochemical activity. However, it was observed that at ZIF-67 concentrations of 2000 and 2500 mg/L, the IpA value decreased. This decrease suggests that increasing the ZIF-67 concentration no longer enhances the electrochemical response, likely due to reduced effectiveness at the electrode surface. Therefore, a concentration of 1500 mg/L was selected as the condition most conducive to the electrochemical response based on the obtained anodic peak current values.

CONCLUSION

In this study, electrodes modified with CS/GQDs/ZIF-67 were prepared and characterized using XRD, FTIR, FE-SEM, and CV. Electrochemical evaluation using CV in PBS at pH 7 showed that the composite's electrochemical activity was influenced by the ZIF-67 composition and the scan rate, reflecting the electron transfer characteristics at the electrode surface. Optimal conditions were observed at a ZIF-67 concentration of 1500 mg/L, which produced the highest anodic peak current response, and a scan rate of 125 mV/s, which provided the most representative response in the electrochemical system observations. However, since the testing was conducted only in a supporting electrolyte without a target analyte or standard redox probe, sensor performance parameters such as selectivity, limit of detection (LOD), limit of quantification (LOQ), and long-term stability have not been evaluated in this study; these aspects need to be further investigated in future research. Thus, this study can be concluded as a preliminary investigation into the basic electrochemical properties of the CS/GQDs/ZIF-67-modified electrode as a material that provides a foundation for further development toward electrochemical sensor applications with more comprehensive evaluation.

REFERENCES

Adeniji, T. M., & Stine, K. J. (2023). Nanostructure modified electrodes for electrochemical detection of contaminants of emerging concern. *Coatings*, *13*(2), 381.

Adeyemi, A. O., & Ojoawo, S. O. (2023). Production and characterization of chitosan of crustacean shells. *Materials Today: Proceedings*, *88*, 128–134.

Ajibade, P. A., & Oloyede, S. O. (2022). Synthesis of metal–organic frameworks quantum dots composites as sensors for endocrine-disrupting chemicals. *International Journal of Molecular Sciences*, *23*(14), 7980.

Alemu, D., Getachew, E., & Mondal, A. K. (2023). Study on the Physicochemical Properties of Chitosan and their Applications in the Biomedical Sector. *International Journal of Polymer Science*, *2023*(1), 5025341.

Amari, A., Elboughdiri, N., Ghernaout, D., Lajimi, R. H., Alshahrani, A. M., Tahoon, M. A., & Rebah, F. Ben. (2021). Multifunctional crosslinked chitosan/nitrogen-doped graphene quantum dot for wastewater treatment. *Ain Shams Engineering Journal*, *12*(4), 4007–4014.

Andani, P. Y. (2017). Zeolite-Modified Carbon Paste Electrode for Determination of Copper Using Anodic Stripping Voltammetry Method. *ALCHEMY Jurnal Penelitian Kimia*.

Bakar, B., Dik, G., Ulu, A., & Ateş, B. (2024). Immobilization of Xylanase into Zeolitic Imidazolate Framework-67 (ZIF-67) and Manganese-Doped ZIF-67 (Mn/ZIF-67): A Comparison Study. *Topics in Catalysis*, *67*(9), 698–713.

Balkanloo, P. G., Sharifi, K. M., & Marjani, A. P. (2023). Graphene quantum dots: synthesis, characterization, and application in wastewater treatment: a review. *Materials Advances*, *4*(19), 4272–4293.

Baranwal, J., Barse, B., Gatto, G., Broncova, G., & Kumar, A. (2022). Electrochemical Sensors and Their Applications: A Review. In *Chemosensors* (Vol. 10, Issue 9).

Ben Aoun, S. (2017). Nanostructured carbon electrode modified with N-doped graphene quantum dots–chitosan nanocomposite: a sensitive electrochemical dopamine sensor. *Royal Society Open Science*, *4*(11).

Bibi, S., Pervaiz, E., & Ali, M. (2021). Synthesis and applications of metal oxide derivatives of ZIF-67: a mini-review. *Chemical Papers*, *75*(6), 2253–2275.

Brasselet, C., Pierre, G., Dubessay, P., Dols-Lafargue, M., Coulon, J., Maupeu, J., Vallet-Courbin, A., de Baynast, H., Doco, T., Michaud, P., & Delattre, C. (2019). Modification of Chitosan for the Generation of Functional Derivatives. In *Applied Sciences* (Vol. 9, Issue 7, p. 1321).

Chen, J., Zhang, T., Xu, Y., Li, H., Cui, H., Zhao, X., Zhou, Y., Qu, K., & Cui, Z. (2025). Molecularly imprinted electrochemical sensor based on MWCNTs/GQDs for the detection of sulfamethazine in aquaculture seawater. *Biosensors*, *15*(3), 184.

Dalal, A., Nehra, K., Hooda, A., Singh, D., Kumar, P., Kumar, S., Malik, R. S., & Rathi, B. (2023). Luminous lanthanide diketonates: Review on synthesis and optoelectronic characterizations. *Inorganica Chimica Acta*, *550*, 121406.

Esmaeilzadeh, M., Sadjadi, S., & Salehi, Z. (2020). Pd immobilized on hybrid of magnetic graphene quantum dots and cyclodextrin decorated chitosan: An efficient hydrogenation catalyst. *International Journal of Biological Macromolecules*, *150*, 441–448.

Garg, N., Kumar, M., Kumari, N., Deep, A., & Sharma, A. L. (2020). Chemoresistive room-temperature sensing of ammonia using zeolite imidazole framework and reduced graphene oxide (ZIF-67/rGO) composite. *ACS Omega*, *5*(42), 27492–27501.

Ghafoor, M., Khan, Z. U., Nawaz, M. H., Akhtar, N., Rahim, A., & Riaz, S. (2023). In-situ synthesized ZIF-67 graphene oxide (ZIF-67/GO) nanocomposite for efficient individual and simultaneous detection of heavy metal ions. *Environmental Monitoring and Assessment*, *195*(3), 423.

Herbei, E. E., Alexandru, P., & Busila, M. (2023). Cyclic Voltammetry of Screen-Printed Carbon Electrode Coated with Ag-ZnO Nanoparticles in Chitosan Matrix. In

Materials (Vol. 16, Issue 8, p. 3266).

Hu, T., Zhang, M., Dong, H., Li, T., Zang, X., Li, X., & Ni, Z. (2022). Free-standing MXene/chitosan/Cu2O electrode: An enzyme-free and efficient biosensor for simultaneous determination of glucose and cholesterol. *Journal of Zhejiang University-SCIENCE A*, *23*(7), 579–586.

Hu, Y., Li, W., Wei, Z., Yang, H., Wang, Y., & Li, S. (2023). Advances in electrochemical sensing with ZIF-67 and related materials. *International Journal of Electrochemical Science*, *18*(7), 100180.

Liu, L., Yang, W., Gu, D., Zhao, X., & Pan, Q. (2019). In situ Preparation of Chitosan/ZIF-8 Composite Beads for Highly Efficient Removal of U(VI). *Frontiers in Chemistry*, *Volume 7-2019*.

Liu, M., Chen, Y., Qin, C., Zhang, Z., Ma, S., Cai, X., Li, X., & Wang, Y. (2018). Electrodeposition of reduced graphene oxide with chitosan based on the coordination deposition method. *Beilstein Journal of Nanotechnology*, *9*(1), 1200–1210.

Marathe, I., Mishra, J., Neelam, N. S., & Tripathi, M. K. (2025). Electrodeposition of multi component alloys for hydrogen evolution reaction–A review. *Next Materials*, *9*, 101023.

Nainggolan, I., Agusnar, H., Alfian, Z., Alva, S., Nasution, T. I., Rahman, R., & Sembiring, A. (2024). Sensitivity of Chitosan Film Based Electrode Modified with Reduced Graphene Oxide (rGO) for Formaldehyte Detection Using Cyclic Voltammetry. *South African Journal of Chemical Engineering*, *48*(1), 184–193.

Nainggolan, I., Martina, S. J., Alva, S., Li, B., Nasution, T. I., Sembiring, A., Duha, A. S., Saisa, S., Rahman, R., & Asrosa, R. (2024). Sensitivity of chitosan/reduced graphene oxide/manganese dioxide modified electrodes for cholesterol detection using cyclic voltammetry. *South African Journal of Chemical Engineering*, *48*, 329–336.

Nainggolan, I., Nasution, T. I., Martina, S. J., Pratama, A., Li, B., Dalimunthe, M. S., Sembiring, A., Sari, R. M., Pasaribu, K. M., Fahri, H., Asrosa, R., Rahman, R., Baidillah, M. R., & Sudarman, S. (2026). A chitosan/rGO/Fe3O4-modified electrode for sensitive cholesterol determination in blood serum. *RSC Adv.*, *16*(31), 28113–28130.

Nasution, T. I., Nainggolan, I., Dalimunthe, D., Balyan, M., Cuana, R., & Khanifah, S. (2018). Humidity detection using chitosan film based sensor. *IOP Conference Series: Materials Science and Engineering*, *309*(1), 12080.

Nesakumar, N., Srinivasan, S., & Alwarappan, S. (2022). Graphene quantum dots: synthesis, properties, and applications to the development of optical and electrochemical sensors for chemical sensing. *Microchimica Acta*, *189*(7), 258.

P, S. A., M, M., & E, M. (2025). Electrochemical detection of sulfamethoxazole antibiotics in water using MXene/ZIF-8 composite modified glassy carbon electrode. *Npj 2D Materials and Applications*, *9*(1), 42.

Salehi, R., Ebrahimian-Hosseinabadi, M., & Rafienia, M. (2025). Fabrication and characterization of polycaprolactone/chitosan/graphene quantum dots nanocomposite scaffolds with potential application in neural tissue engineering. *Carbon Trends*, *21*, 100595.

Sarhan, H.-A., Fathy, N., El-Sakhawy, M., & Kamel, S. (2022). Boosting the adsorption capacity and photocatalytic activity of activated carbon by graphene quantum dots and titanium dioxide. *Diamond and Related Materials*, *132*, 109640.

Shahsavari, M., Mortazavi, M., Tajik, S., Sheikhshoaie, I., & Beitollahi, H. (2022). Synthesis and Characterization of GO/ZIF-67 Nanocomposite: Investigation of Catalytic Activity for the Determination of Epinine in the Presence of Dobutamine. In *Micromachines* (Vol. 13, Issue 1, p. 88).

Shahzaib, A., Ahmad, I., Alshehri, S. M., Ahamad, T., & Nishat, N. (2024). Green synthesis of ZIF-67 composite embedded with magnetic nanoparticles and ZnO decoration for efficient catalytic reduction of rhodamine B and methylene blue. *Chemistry of Inorganic Materials*, *2*, 100037.

Sun, S., Tang, Y., Wu, C., & Wan, C. (2020). Phytic acid functionalized ZIF-67 decorated graphene nanosheets with remarkably boosted electrochemical sensing performance. *Analytica Chimica Acta*, *1107*, 55–62.

Thai, V.-A., Nguyen, T.-B., Huang, C. P., Bui, X.-T., Doong, R., Chen, C.-W., & Dong, C.-D. (2023). Graphene quantum dots (GQDs) decorated zeolitic imidazole framework-67 (ZIF67) electrode for the in-situ oxidation of ciprofloxacin in water. *Environmental Technology & Innovation*, *30*, 103039.

Zhang, L., Zhu, J., Hong, W., & Li, G. (2024). Highly sensitive electrochemical detection of cholesterol based on Au–Pt NPs/PAMAM–ZIF-67 nanomaterials. *Analytical Sciences*, *40*(1), 37–45.